Zeitschrift: IABSE reports = Rapports AIPC = IVBH Berichte

Band: 60 (1990)

Artikel: Behavior of concrete encased steel frames with reinforced concrete walls

Autor: Goto, Tetsuro / Hirosawa, Masaya

DOI: https://doi.org/10.5169/seals-46520

Behavior of Concrete Encased Steel Frames with Reinforced Concrete Walls

Comportement des charpentes en acier enrobé de béton avec murs en béton armé

Tragverhalten von Stahl-Beton-Verbundrahmen mit Stahlbetonwänden

Tetsuro GOTO
Senior Res. Eng.
Building Res. Inst.
Tsukuba, Japan

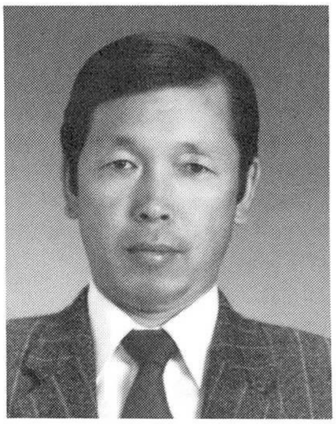

Tetsuro Goto has been actively engaged in research in concrete structures and earthquake-resistant design. In 1978, he was awarded a prize by the Japan Concrete Institute for his study.

Masaya HIROSAWA
Dep. Dir. Gen.
Building Res. Inst.
Tsukuba, Japan

Masaya Hirosawa received his doctor of engineering degree at the University of Tokyo. His research has focused on concrete structures. In 1985, he was awarded a prize by the Architectural Institute of Japan for his study.

SUMMARY

This paper describes an experimntal test of the stiffness, horizontal bearing capacity, deformation capability, and failure mechanism of Concrete Encased Steel frames containing a reinforced concrete wall. The stiffness and maximum horizontal bearing capacity are higher than those of a simple Concrete Encased Steel frame. When the frame containing a wall is deformed greatly, the wall fails and the structural behavior becomes similar to that of a simple frame.

RÉSUMÉ

Cet article décrit une série d'essais sur la rigidité, la force portante horizontale, la résistance à la déformation et les mécanismes de rupture des charpentes en acier enrobé de béton comportant un mur en béton armé. La rigidité et la force portante maximum sont supérieures à celles d'une simple charpente en acier enrobé de béton. Quand une charpente en acier enrobé de béton avec mur en béton armé se déforme de manière notable, le mur cède et le comportement structurel devient identique à celui d'une simple charpente en acier enrobé de béton.

ZUSAMMENFASSUNG

Dieser Artikel beschreibt eine Experimentalprüfung der Biegefestigkeit, der Tragfähigkeit, des Widerstandes gegen die Formveränderung und des Verhaltens bei einem Notfall bedingt durch Stahlbetonrahmen die eine Stahlbetonwand enthalten. Die Biegefestigkeit und die maximale Tragfähigkeit sind höher als jene von einem reinen Stahlbetonrahmen. Werden die Verformungen des Stahlbetonrahmens mit der Wand gross, so versagt die Wand und der Rahmen verhält sich ähnlich einem Rahmen ohne Wand.

1. INTRODUCTION

The SRC frame is suitable for various purposes because it is very ductile. This paper describes a seismic resistance test in an attempt to establish a design method for SRC frames used as part of the composite structure of medium- to high-rise apartment buildings. H-shaped steel and reinforcement are incorporated in concrete to form an SRC frame consisting of columns and beams. To use buildings as shelters, a thin concrete wall with a single reinforcing bar with openings is incorporated in the SRC frame. This composite structure has been used for many buildings in the past and will be used more often in the future. However, there are still many unsolved points concerning the lateral stiffness, maximum horizontal bearing capacity, failure mechanism, and deformation capability of frames that contain a wall with openings. In this study, we planned a frame experiment as the first step toward establishing a method by which to evaluate the unsolved points.

2. EXPERIMENTAL PROGRAM

2.1 Specimens

An 11-story apartment building with side corridors which was designed according to [1] is used as a model for specimen design. From ten spans in the longitudinal direction of the building, the central two spans of the lowest three stories are taken and reduced in half. Three specimens are used. Figures 1 to 6 show the shape and structure of the specimens. Table 1 lists the cross sectional dimensions of the columns and beams. Each specimen is 6.9 m high and 8.7 m long. Column and beam members of each specimen are incorporated in an SRC frame and has the same specifications. The depth of the column on the first floor is 42.5 cm and the width 35 cm. The depth of the column on the second floor is 37.5 cm and the width 22.5 cm.

Specimen No.1 is a pure frame without the non-seismic reinforced concrete wall, so that the difference of the deformation capability between structures with and without a wall can be analyzed. Specimen No.2 contains a reinforced concrete wing wall at the side of the SRC frame. Specimen No.3 contains a reinforced concrete wall with several large and small openings. The typical opening shape that can be seen in many apartment buildings is sampled and tested; special shapes are not considered. The wall thickness is 1/6 of the width of the column because the walls of many apartment buildings are about this thickness. Table 2 shows the results of the material test.

2.2 Loading Method

Figure 7 outlines load application. Four 686 KN actuators, producing horizontal load (Q), are set on top of the specimens. Horizontal load is applied statically in positive and negative directions for 17 cycles with small to large deflections (Figure 7). The angle of rotation of members for horizontal loading control is the value obtained by dividing the target horizontal deflection (δ_T) by the distance (H) between the base of the column on the first floor and the loading point ($R_T \fallingdotseq \delta_T/H$ rad).
Axial force of 5884 KN/m^2 equivalent to the sustained loading is applied to

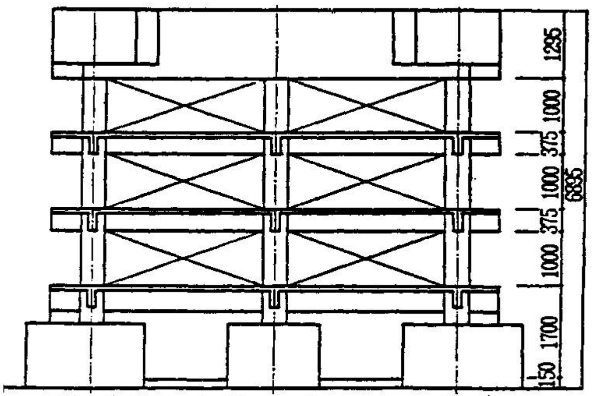

Fig 1 Description of specimen No.1

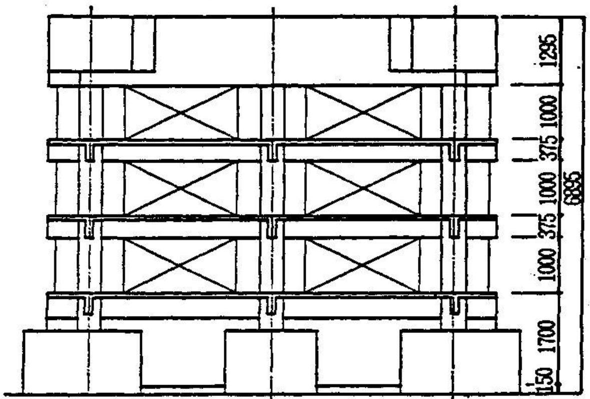

Fig 3 Description of specimen No.2

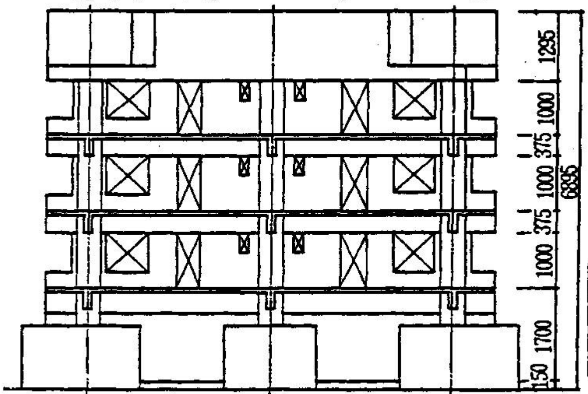

Fig 5 Description of specimen No.3

Table 2 Member list of SRC frame

		Column	Beam	
		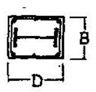 $Z_3 \sim Z_1$	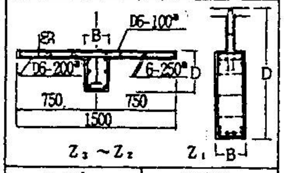 $Z_3 \sim Z_2$ Z_1	
			end	center
Z_3	B×D	300×425	225×375	225×375
	Flg.	PL-9×100	PL-16×100	PL-16 ×100
	Web	PL-9	PL-4.5	PL-3.2
	Main bar	4-D13, 2-D10	4-D13, 2-D13	2-D13, 2-D10
Z_2	B×D	325×425	225×375	225×375
	Flg.	PL-12 ×100	PL-16×100	PL-16 ×100
	Web	PL-6	PL-4.5	PL-3.2
	Main bar	4-D13, 2-D10	3-D13, 2-D10	2-D13, 2-D10
Z_1	B×D	350×425	300×1250	300×1250
	Flg.	PL-16 ×100	———	———
	Web	PL-9	———	———
	Main bar	4-D13, 2-D10	10-D16, 10-D16	6-D16, 6-D16
Hoop[Z_3:D10-@50, $Z_2 \sim Z_1$:D6-@50] Stirrup[D6-@100]				

unit : mm

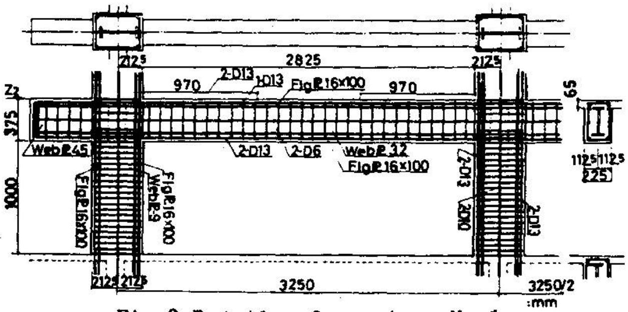

Fig 2 Details of specimen No.1

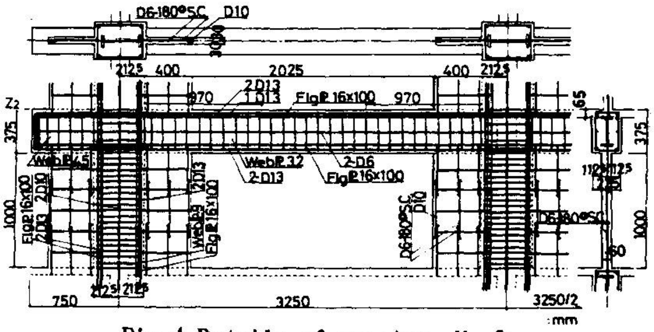

Fig 4 Details of specimen No.2

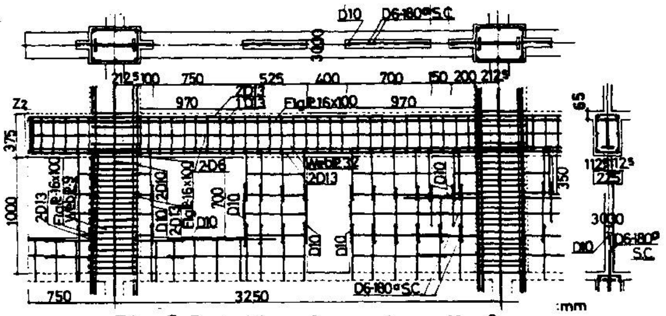

Fig 6 Details of specimen No.3

Table 1 Mechanical properties

Steel (N/mm²)	web (3.2)	web (4.5)	web (6.0)	web (9.0)	Flange (12.0)	Flange (16.0)	D6	D10	D13
σ_y	330	249	346	334	288	280	300	427	364
σ_t	407	373	449	479	438	449	450	597	520
$E_c \times 10^3$	208	215	213	201	212	214	188	186	180

Concrete :
[NO.1 σ_c =24.2 N/mm², σ_t =1.89 N/mm², Ec =2.13×10⁴ N/mm²)
[NO.2 σ_c =24.2 N/mm², σ_t =1.82 N/mm², Ec =2.13×10⁴ N/mm²)
[NO.3 σ_c =25.0 N/mm², σ_t =1.93 N/mm², Ec =2.16×10⁴ N/mm²)

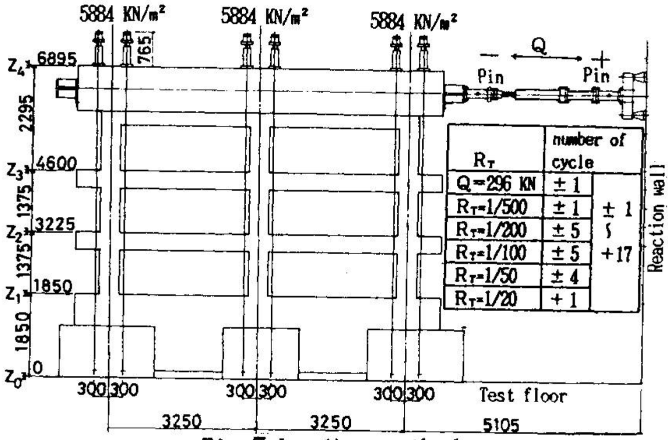

Fig 7 Loading method

the top of the specimens. This force is kept at a constant level during horizontal loading. The total measurement items per specimen amounted to 600, including horizontal and vertical deflection, and H-shaped steel strain. The progress of failure was photographed and sketched.

3. EXPERIMENT RESULTS AND REVIEW

3.1 Relationship between failure development and horizontal loading deflection

Figure 8 shows the relationship between horizontal deflection and horizontal load measured along the center of the beam on the top of specimen No.1. Figure 9 shows the failure condition at the end of the experiment in which $R_T \fallingdotseq 1/20$ was reached. Figures 10 to 13 show the results of the same experiment for specimens No.2 and No.3.

In specimen No.1, bending crack (BC) occurred in the column bottoms on the first floor, in the beams on the second and third floors, and in the column tops on the third floor at $Q \fallingdotseq 235$ KN to 294 KN. At $R_T \fallingdotseq 1/200$, BC occurred in the columns and beams on all the floors, and bending and shear crack (BSC) and shear crack (SC) occurred in all the members. At $R_T \fallingdotseq 1/100$, the column tops on the third floor, the column bottoms on the first floor, and the beam steel of the center columns on all the floors yielded. At the cycle of the same R_T, the column tops on the third floor, the column bottoms on the first floor, and the beam ends on all the floors began to be crushed. At $R_T \fallingdotseq 1/50$, the maximum load of 1153.3 KN was measured. After repetition of $R_T \fallingdotseq 1/50$, crushing of the column tops on the third floor and the column bottoms on the first floor progressed. The final failure mode of specimen No.1 showed a flexural failure type.

In specimen No.2, at $Q \fallingdotseq 235$ KN to 294 KN, BC occurred in the column ends on all the floors. Before $R_T \fallingdotseq 1/500$ was reached, BC occurred in the column tops on the third floor, and BC and SC occurred in the wing walls on all the floors. BSC progressed before $R_T \fallingdotseq 1/200$ was reached. At the fifth cycle of the same R_T, the column tops on the third floor and the wing wall of the column bottoms on the first floor were crushed. At $R_T \fallingdotseq 1/50$, the maximum load of 1357.7 KN was measured. At the first to fifth cycles of $R_T \fallingdotseq 1/100$, crushing of the wing walls near the column tops on the first and second floors progressed. At $R_T = 1/50$, crushing of the wing wall of the column top and the beam ends on the third floor progressed. The final failure mode of specimen No.2 was almost the same as that of specimen No.1.

In specimen No.3, at $Q \fallingdotseq 392$ KN, BC occurred in the beam ends on the second floor. At 412 KN, SC occurred. When R_T reached 1/500, SC occurred in the walls on all the floors. At $R_T \fallingdotseq 1/200$, when the maximum load of 1463.6 KN was measured, shear failure occurred in some walls. At the fifth cycle of the same R_T, shear failure occurred in the walls on all the floors. At $R_T \fallingdotseq 1/100$ and $R_T \fallingdotseq 1/50$, crushing of the column tops on the third floor, the column bottoms on the first floor, and the beam ends on all the floors progressed. The final failure mode of specimen No.3 was almost the same as that of specimens No.1 and No.2.

The failure mode of the pure frame was a bending failure. The final failure

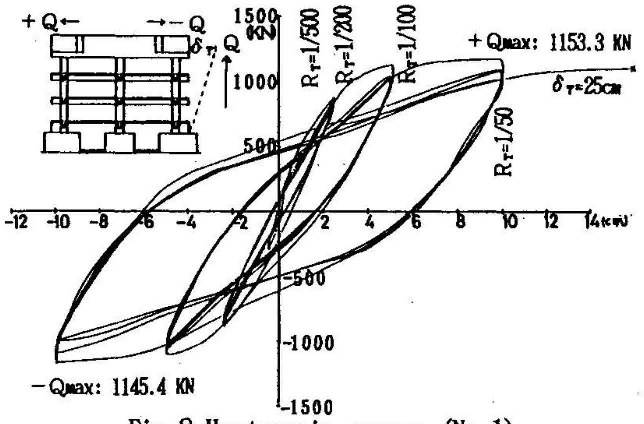

Fig 8 Hysteresis curves (No.1)

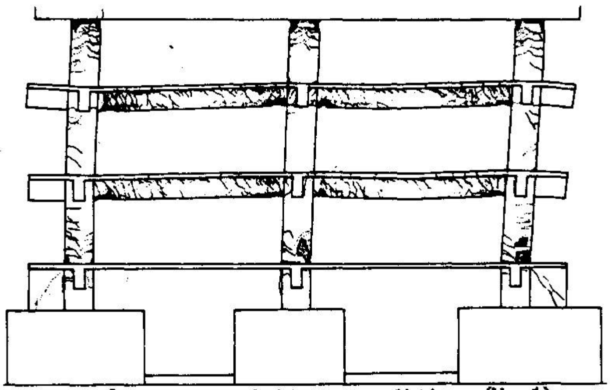

Fig 9 Ultimate failure condition (No.1)

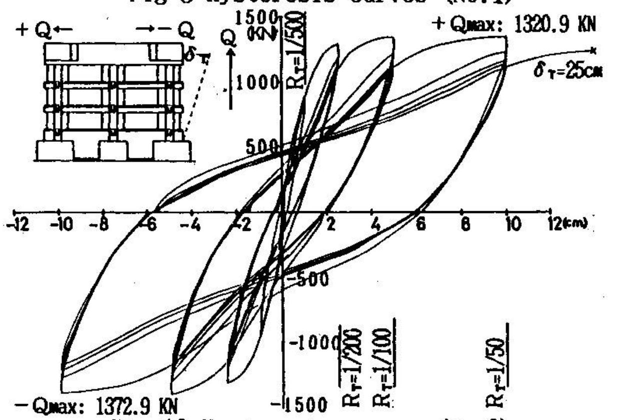

Fig 10 Hysteresis curves (No.2)

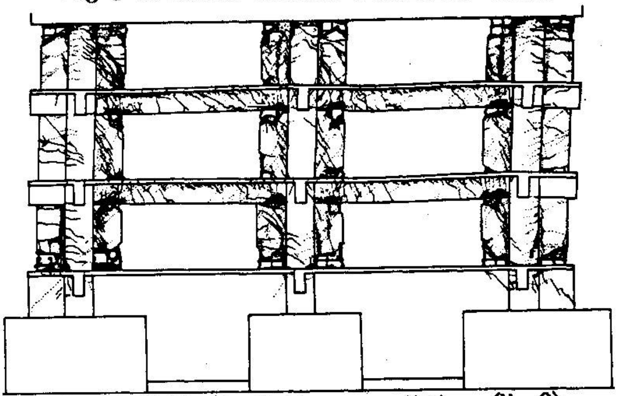

Fig 11 Ultimate failure condition (No.2)

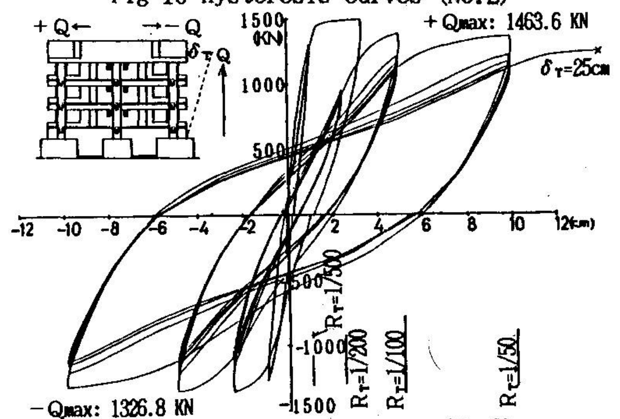

Fig 12 Hysteresis curves (No.3)

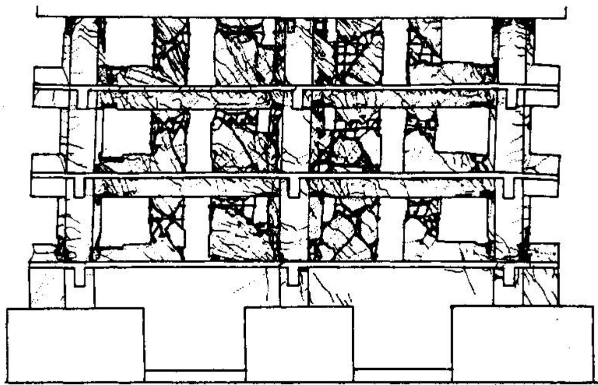

Fig 13 Ultimate failure condition (No.3)

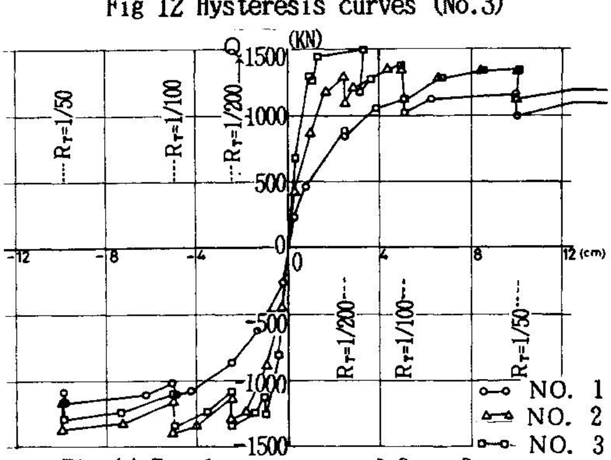

Fig 14 Envelope curves of Q - δ_T curves

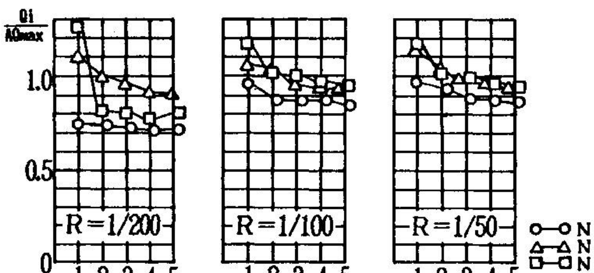

Fig 15 Specimen 1: Based on maximum horizontal load, horizontal load at each cycle

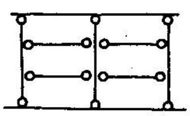

Fig 16 Position where yield hinge of SRC frame is formed

mode of the frame containing a reinforced concrete wall was the same as that of the pure frame. Although the frame contained a wall, the wall did not affect the peripheral frames much. The axial force of 5884 KN/m^2, applied to each column, could be kept at this level until the end of the test.

3.2 Deflection behavior and horizontal bearing capacity

Figure 14 shows an envelope of $Q - \delta_T$ curve. From this figure, we can see that the reinforced concrete wall greatly affected the lateral stiffness of the SRC frame. The measured elastic stiffness of the frame containing a wing wall was about double the elastic stiffness of the pure frame, and about five times that of the frame containing a wall with openings. A beam theory can be established to analyze the stiffness of a reinforced concrete wall if a model for the wall with openings is carefully made.

The deflection behavior of each specimen showed a stable load-deflection curve up to $R_T \fallingdotseq 1/50$. Each specimen, deformed up to $R_T \fallingdotseq 1/20$, showed a deflection curve of relatively little decrease in the bearing capacity. It can be said that each frame had sufficient ductility.

Figure 15 shows the bearing capacity ratio based on the maximum horizontal bearing capacity of specimen No.1. When deformed greatly, specimens No.2 and No.3 had the same bearing capacity as that of specimen No.1.

If the maximum horizontal bearing capacity of the pure frame is assumed to be 1, the capacity for the frame containing a wing wall was 1.19, and the capacity for the frame containing a wall with openings was 1.32. The frame containing a reinforced concrete wall improved the maximum bearing capacity. Also a virtual work method can be used to predict the maximum bearing capacity. Figure 16 shows the frame failure mode. The bearing capacity of specimen No.1, obtained by the virtual work method, was about 80% of the experiment value of the maximum horizontal bearing capacity.

4. CONCLUSIONS

From this experiment it was found that, concerning the elastic and plastic behaviors, the stiffness and horizontal bearing capacity of the SRC frame containing a reinforced concrete wall was higher than those of the pure frame. It was feared that the wall worsens the structural performance of the SRC frame. By the time the frame was deformed greatly, it showed almost the same behavior as that of the pure frame. This is because the SRC frame has sufficient structural performance. If sufficient stiffness is sustained to secure the building use and living performance, the deflection caused by an earthquake can be kept small. Even if a wall is destroyed by a big earthquake, the structure of the SRC frame is safe against collapse. If a shear failure occurs, it may be impossible to open or close doors. One way to avoid this problem is to install doors away from the columns and beams.

REFERENCE

[1] SRC Design Standard, Architectural Institute of Japan, 1987.